SLAC-PUB-103
April 1965

PHOTOPRODUCTION OF MUON PAIRS*

by

Allan S. Krass
The University of California, Santa Barbara
Santa Barbara, California

ABSTRACT

The virtual Compton corrections to muon pair production are analyzed and compared with the Bethe-Heitler cross section for symmetric pairs. The three corrections studied are the peripheral, diffraction and "compound state" processes. It is shown that the peripheral processes will be the first to give significant corrections as the photon energy and muon detection angle are increased in future experiments. It is predicted that mu-pair experiments should be interpretable as pure Bethe-Heitler processes (and therefore valid tests of QED) up to photon energies of 10 BeV and muon angles of 18° in the lab system.

(Submitted to the Physical Review)

---

*Work done at the Stanford Linear Accelerator Center, Summer 1964, and supported by the U.S. Atomic Energy Commission.

I. INTRODUCTION

It has long been known[1] that the production of pairs of electrons or muons with wide angular separations could serve as a probe for testing quantum electrodynamics at small distances. The object of the experiment is to measure processes in which a virtual electron or muon is very far off its mass shell so that deviations from QED which involve the fermion propagator might be observed.

The standard experiment involves the diagrams of Fig. 1, and it has been customary to observe the muons symmetrically about the forward direction in order to eliminate interference from the so-called Compton diagrams of the class indicated by Fig. 2.

It is of course extremely important to know that the effects of such Compton diagrams are negligible if one is to be able to interpret experimental deviations from the predictions of the Bethe-Heitler graphs as a breakdown of QED. It is the purpose of this paper to examine the Compton contributions in detail to try to set limits on how far these experiments may be pushed.

Recent experiments[2] at the Cambridge Electron Accelerator have used photon energies (k) of nearly 5 BeV and muon angles of up to $\theta = 10^{\circ}$ in the lab system. This gives a mass for the virtual muon of about 0.6 BeV. Experiments proposed[3] for the Stanford Linear Accelerator will use k = 10 BeV and $\theta \approx 20^{\circ}$, which lead to a muon mass of 2.1 BeV. Some estimates will be made of the Compton effects which will treat the energy and angular ranges spanned by these two experiments.

The paper is organized as follows: In Sec. II the exact Bethe-Heitler cross section is written down and certain kinematical and experimental problems are discussed. In Sec. III the Compton contributions are estimated, and in Sec. IV the conclusions are summarized.

II. BETHE-HEITLER CROSS SECTION

We have evaluated the cross section[4] from the graphs of Fig. 1 assuming arbitrary energies and angles for the final muons. All muon mass terms have been kept and recoil has been treated exactly. All of these contributions are important for the experiments we will consider. The following invariant quantities are used:

$$\sigma = (p_+ + p_-)^2$$

$$t = q^2 = (k - p_+ - p_-)^2 = (Q - Q')^2$$

$$W^2 = (k + Q)^2 = (p_+ + p_- + Q')^2$$

$$v = 2(p_+ - p_-) \cdot k$$

$$w = 2(p_+ - p_-) \cdot P$$

where $P = Q + Q'$ (the sum of the initial and final proton four-momenta).

We denote by $\left[|T|^2_{BH}\right]$ the invariant matrix element squared and averaged over initial spins and summed over final spins.

$$\left[|T|^2_{BH}\right] = \frac{e^6}{4m_\mu^2 t^2} (A + m_\mu^2 B) \qquad (1)$$

$$A = -2\mathcal{F}_1 \left\{\frac{(\sigma+t)^2 + v^2}{(\sigma-t)^2 - v^2}\right\} - t\mathcal{F}_2 \left\{\frac{(4kM-\sigma+t)^2 + w^2}{(\sigma-t)^2 - v^2}\right\} \qquad (2)$$

$$B = \frac{(F_1+\mu F_2)^2}{M^2}\left\{\frac{16m^2t - (\sigma+t+v)^2 + 6t(\sigma+t+v)}{(\sigma - t + v)^2} + \frac{16m^2t - (\sigma+t-v)^2 + 6t(\sigma+t-v)}{(\sigma - t - v)^2}\right.$$

$$\left. - 2\,\frac{16t(\sigma-t-m^2) - (\sigma-t)^2 + v^2}{(\sigma-t)^2 - v^2}\right\} + \mathcal{F}_2\left\{\frac{(4kM+t-\sigma-w)^2 + 2P^2(\sigma+t+v)}{(\sigma-t+v)^2}\right.$$

$$\left. + \frac{(4kM+t-\sigma-w)^2 + 2P^2(\sigma+t-v)}{(\sigma-t-v)^2} - 2\,\frac{(4kM-\sigma+t)^2 + 4P^2(\sigma-2t) - w^2}{(\sigma-t) - v^2}\right\} \qquad (3)$$

In the above equations $\mathcal{F}_1$ and $\mathcal{F}_2$ are the combination of F_1 and μF_2 which were defined by Bjorken, Drell and Frautschi:[5]

$$\mathcal{F}_1 = \frac{t}{M^2}\,(F_1 + \mu F_2)^2 + \frac{P^2}{2M^2}\left(F_1^2 - \frac{t}{4M^2}\,\mu^2F_2^2\right) \qquad (4)$$

$$\mathcal{F}_2 = \frac{1}{M^2}\left(F_1^2 - \frac{t}{4M^2}\,\mu^2F_2^2\right) . \qquad (5)$$

To obtain the symmetric amplitude from Eqs. (1) and (3) simply set $v = w = o$.

Using Eq. (1) and (3) and the representations given by Hand, Miller and Wilson[6] for the proton form factors, we have calculated the symmetric Bethe-Heitler cross section for a range of energies and angles. The cross section is

$$\frac{d\sigma}{d\epsilon_+ d\epsilon_- d\theta_+ d\theta_- d\varphi_+ d\varphi_-} = \frac{M\epsilon^2 \sin^2\theta}{k^2[M-2\epsilon(1-\cos\theta)]}\,\frac{\alpha^3}{4\pi^2}\,\frac{1}{t^2}\,(A + m^2 B) \qquad (6)$$

where we have assumed that both muons are detected and resolved in energy and angle. This has necessitated dividing out the bremsstrahlung spectrum to get the cross section per equivalent quantum.

Although Fig. 3 gives a very accurate[7] value for the symmetric Bethe-Heitler cross section, it is possible that this number could be misleading when comparisons are made with the Compton contributions. Because any experiment will have finite resolution in the six muon energy and angle variables, the cross section of Eq. (6) must be integrated over these variables. A few numerical examples have shown that the Bethe-Heitler cross section and the ratio of Bethe-Heitler to Compton processes are fairly sensitive to the resolution. We have not worked out any examples because a proper six-dimensional integration would take more computer time than is presently at our disposal, but such integrations can easily be done as particular experiments are designed.

Finally, it should be pointed out that we have assumed hydrogen as the target as opposed to carbon which was used in the CEA experiment.[2] Our calculation will apply to experiments in which the momentum transfer to the proton becomes quite large relative to its binding energy in carbon. For these experiments coherence effects would be negligible and the presence of a carbon nucleus would be more of a nuisance than an aid.

III. COMPTON CORRECTIONS

All of these processes involve the virtual Compton scattering of a photon followed by the decay of the time-like photon into a μ^+-μ^- pair. The three possible ways in which Fig. 2 can be broken up are shown in Fig. 4. Figure 4a includes among others, the peripheral or one-pion exchange processes and the diffraction or two-pion

exchange processes. We will consider only these two contributions to Fig. 4a.

In each of the graphs of Fig. 4 the virtual photon is coupled to a vertex involving strongly interacting particles. We handle this situation in the standard manner, assuming that the photon communicates with the vertex via the ρ, ω, and φ mesons.

A. Peripheral

In the peripheral case we get Fig. 5. In the spirit of the peripheral approach we assume that the pion couples to the proton and γ-ρ currents as if it were real, and we expect this to be a good approximation for momentum transfers less than a few pion masses.

If we denote by $\left[\left|T_{per}\right|^2\right]$ the matrix element of Fig. 5 summed and averaged over spins, we obtain[7]

$$\left[\left|T_{per}\right|^2\right] = \frac{1}{2^8} \frac{g_{\pi NN}^2 e^4}{m_\mu^2 M^2} \left(\frac{t}{\sigma}\right) \left(\frac{t-\sigma}{t-m_\pi^2}\right)^2 \times \left[\frac{g_{\rho\pi\gamma}}{\gamma_\rho} \frac{m_\rho}{\sigma - m_\rho^2 + i\Gamma_\rho m_\rho}\right.$$

$$\left. + \frac{g_{\omega\pi\gamma}}{\gamma_\omega} \frac{m_\omega}{\sigma - m_\omega^2 + i\Gamma_\omega m_\omega} + \frac{g_{\varphi\pi\gamma}}{\gamma_\varphi} \frac{m_\varphi}{\sigma - m_\varphi^2 + i\Gamma_\varphi m_\varphi}\right]^2 \qquad (7)$$

If the experiment is performed at energies and angles which put σ at the real mass of one of the resonances one expects a strong enhancement and a greater chance of seeing these peaks in the measured cross section. This possibility is further analyzed in Sec. IV.

We now consider the ratio R of the peripheral cross section to the Bethe-Heitler cross section. In Fig. 6, R is plotted for a wide range

of energies and angles. For very low momentum transfer t, R becomes small since T_{per} is proportional to t and T_{BH} goes as t^{-2}. We expect R to increase rapidly as t increases; in Fig. 6 we have indicated the momentum transfers at which R passes through 10% for four energies. From Fig. 6 we see that an angle of 18° in the lab at a photon energy of 10 BeV is possible before the peripheral corrections exceed 10%. This corresponds to the virtual muon having a mass of about 2.1 BeV.

We must now examine the validity of a peripheral approximation at these energies and angles. We are assuming that the photoproduction of ρ mesons is largely peripheral for momentum transfers less than about 0.45 $(\text{BeV}/c)^2$ and photon energies greater than 3 BeV. We have also dropped the ω intermediate state on the assumption that the $\gamma\pi\omega$ coupling is substantially smaller than the $\gamma\pi\rho$ coupling. The data of Crouch[9] et al. is consistent with these assumptions when real ρ's are produced.* As a function of σ, the amplitude of Fig. 5 goes as σ^{-1} for t fixed and σ large. This is true because the two propagators for the virtual ρ and virtual γ provide enough powers of σ to more than cancel the energy dependence introduced by the gauge invariant coupling:[7]

$$\epsilon_{\mu\nu\lambda\sigma}\, \epsilon^{\mu}(\gamma)\, k^{\nu}\, \epsilon^{\lambda}(\rho) p^{\sigma} \qquad (8)$$

However, we must also consider the σ dependence of the form factor at the $\rho\pi\gamma$ vertex. We have used the graphs of Fig. 7 to get a qualitative estimate of the vertex function. The sum of the two graphs in Fig. 7 leads to a form factor which, after one subtraction is used to renormalize to one at $\sigma = m_{\rho}^2$ and $t = m_{\pi}^2$, still increases logarithmically

*See note added in proof, p. 14.

for large σ or large t. Therefore, on the basis of these diagrams we might expect the peripheral contribution to grow somewhat faster than it does in Fig. 6. But again the σ and t dependences come from the coupling at the $\rho\pi\gamma$ vertex. If we could find some way to treat the $\gamma \to 3\pi \to \rho\pi$ vertex without coupling to vector particles, the energy dependence would be more favorable. We conclude that the contribution of the $\rho\pi\gamma$ vertex cannot be definitely determined but it seems safe to say that at worst it introduces an extra log σ or log t factor. This will not have a very significant effect on our conclusions.

B. Diffraction

In discussing the diffraction contribution we need only consider the process of photoproduction of ρ mesons. The subsequent "decay" of the ρ into a photon and then a muon pair will lead to a common factor which will multiply all ρ-production amplitudes.

The most recent data[9] on the photoproduction of ρ's is consistent with one-pion exchange for $t \lesssim 0.4$ (BeV/c)^2 and $\omega > 1.4$ BeV, but on the other hand the experimenters have not been able to exclude diffraction as a possible major contributor. We will handle diffraction in the same way as Drell and Berman,[8] i.e., replacing the top rung of the diffraction graph for pion-nucleon scattering by the rung shown in Fig. 8.

The result of this calculation is

$$\left[|T|^2_{\text{Diff}}\right] = \frac{p_\rho}{\epsilon_\rho} \frac{1}{16} \frac{\left(\frac{g^2_{\gamma\pi\omega}}{4\pi}\right)\left(\frac{g^2_{\rho\pi\omega}}{4\pi}\right)}{\left(12\,\Gamma_\rho/m_\rho\right)^2} \left[2\,\frac{\sigma - t}{m_\omega^2} - 1\right]^2 e^{at} \left(\frac{d\sigma}{d\Omega}\right)_{\pi N} \qquad (9)$$

where as usual the mass of the final ρ is $\sigma^{\frac{1}{2}}$ and where the intermediate ω is on its mass shell as required by the diffraction approach. The form of the πN diffraction cross section is taken from the data of Ting, Jones and Perl.[10]

The ratio of the diffraction amplitude to the peripheral amplitude given by

$$\left[|T|^2\right]_{per} = \frac{1}{2^4} \frac{g^2_{\rho\pi\gamma}\, g^2_{\pi NN}}{M^2} \left(\frac{t}{m_\rho^2}\right)\left(\frac{t-\sigma}{t-m_\pi^2}\right)^2 \qquad (10)$$

can now be evaluated, and if one assumes that $g_{\omega\pi\gamma} = g_{\rho\pi\gamma}$ and that

$$\frac{g^2_{\rho\pi\omega}}{4\pi} \approx 2$$

it is found that the diffraction contribution is at most equal to the peripheral contribution at essentially all the energies and angles of interest. We feel, however, that this is probably an overestimate because $g_{\omega\pi\gamma}$ seems to be significantly smaller than $g_{\rho\pi\gamma}$ [9] and the value of $g_{\rho\pi\omega}$ is an upper limit.[8] However, as the muon angles get large and t begins to increase more rapidly, the exponential causes the diffraction amplitude to fall behind the peripheral, and diffraction is no problem at all at the larger muon angles.

Our conclusion is that, even if ρ production proceeds largely by diffraction instead of one-pion exchange, our estimates of the energies and angles at which the Bethe-Heitler terms dominate are, at worst, unchanged, and may possibly be conservative.

C. Direct S-Channel Processes

Another possible mechanism for ρ production is the one illustrated by Figs. 4b and 4c. The photon and proton form some "compound state" which decays to a ρ and proton. In a dispersion treatment one would assume that the effects of this compound state could be approximated by a set of poles at the nucleon isobars. This involves the assumption that the $\gamma p \rightarrow \rho p$ matrix element satisfies an unsubtracted dispersion relation and that this dispersion relation remains valid even when the final ρ is taken far off its mass shell. If these assumptions are made it is not difficult to prove that these resonance contributions to mu-pair production are completely negligible. However, it is very difficult to justify these assumptions, and we have chosen to make another argument which relies entirely on experimental observations.

Referring to the data of Ref. 9, in particular Fig. 2, we find a very strong peaking of the ρ cross section in the forward direction. This is most evident in the angular distribution of the recoil protons. If compound states with reasonable angular momenta were contributing we would expect to see ripples in the angular distribution and a backward peak. Although such behavior cannot be ruled out, it seems safe to say that it must contribute substantially less than 25% of the cross section.

We can obtain an overestimate of the contribution of compound states to the differential cross section for ρ production in the forward direction by making the following two assumptions:

(a) Compound states account for 25% of the total ρ production cross section.

(b) The process proceeds through a single angular momentum channel - say $\ell = 2$. We choose this value of ℓ because it gives a large estimate for the ratio of the differential cross section in the forward direction to the total cross section. In fact we have the relation[11]

$$\left(\frac{d\sigma}{d\Omega}\right)_o = \frac{2\ell + 1}{4\pi} \sigma_{total} \tag{11}$$

which holds in the center-of-mass system for any reaction which goes via a single ℓ channel.

We will assume $\sigma_{total} \approx 7.5$ μb for these compound processes[12] in the following calculation. This leads to

$$\left(\frac{d\sigma}{d\Omega}\right)_{o_{CM}} \approx 4 \text{ μb/sr} \tag{12}$$

in the center-of-mass system. Converting this to the lab system, we find:

$$\left(\frac{d\sigma}{d\Omega}\right)_{o_{lab}} = \frac{P_{lab}}{P_{CM}} \frac{W^2}{E_{CM}\left[M + k_{lab}\,(1-\beta_\rho^{-1})\right]} \left(\frac{d\sigma}{d\Omega}\right)_{o_{CM}} \tag{13}$$

where E_{CM} is the center-of-mass energy of the initial proton ($E_{CM} = \gamma M$) and β_ρ is the velocity of the final ρ in the lab. Using standard Lorentz transformation formulae and assuming that the ρ is highly relativistic in both the lab and center-of-mass, we get:

$$\left(\frac{d\sigma}{d\Omega}\right)_{o_{lab}} = \frac{W^2}{M^2} \left(1 + \frac{k}{k+M}\right) \left(\frac{d\sigma}{d\Omega}\right)_{o_{CM}} \tag{14}$$

which leads to:

$$\left[|T|^2\right]_{\text{compound}} \approx 32\,\pi^2 \left(\frac{W}{M}\right)^2 \left(\frac{d\sigma}{d\Omega}\right)_{\theta_{CM}} \qquad (15)$$

for large k.

When Eq. (15) is compared with Eq. (10) for various energies and angles, it is found that for small momentum transfers where the peripheral cross section is small, the compound state contribution can be a factor of three larger than the peripheral. But it cannot be big enough to be seen over the Bethe-Heitler events. As t increases to the point where the peripheral can be seen, the compound contribution, being independent of t, becomes negligibly small. Thus we conclude that contributions from resonant states are almost certainly negligible for all proposed energy and angle regions.

IV. CONCLUSIONS

The results of the preceding analysis can be summed up as follows: The most troublesome Compton process is the peripheral, which will become large enough to significantly affect the cross section at momentum transfers of about 0. (BeV/c)^2 when the incident photon has an energy of 10 BeV. This estimate is based on the data of Ref. 9 and the assumption that the peripheral model is valid up to the momentum transfers mentioned. Any corrections to the peripheral model would probably take the form of distorted incoming and outgoing waves due to initial and final state interactions. These effects have been considered by Gottfried and Jackson[13] and Ross and Shaw[14]; in general the effect is to reduce the

cross section below the value predicted by the peripheral model. The reduction is greater at higher momentum transfers.

These effects, if present, will clearly cause our estimates of the range of validity of the Bethe-Heitler formula to be too conservative.

If the production of ρ's goes via a diffraction mechanism or via intermediate resonance states we have shown that the effects will be less than the peripheral. Therefore, in any event it seems reasonable to conclude that one will be able to observe the pure Bethe-Heitler process for values of the virtual muon mass in excess of 2 BeV. This will test the limits of quantum electrodynamics to distances of the order of 0.3×10^{-14} cm, which is a factor of five better than existing measurements.

In closing, we would like to discuss the possibility of observing the ρ and ω resonances as bumps in the μ-pair cross section.[8] If Eq. (7) is analyzed it is found that the best chance for observing this effect occurs at relatively low photon energies (3-4 BeV) and relatively large angles (11°-14°). If the ρ and ω are assumed to couple equally at the $\gamma\pi$ vertex and if the resolution is sufficiently good, one can get the peripheral contribution to about 30 or 40% of the Bethe-Heitler contribution, which would make the bump just barely visible.

The most important assumption in the above is the equality of $g_{\rho\pi\gamma}$ and $g_{\omega\pi\gamma}$. If, as seems to be the case,[9] $g_{\omega\pi\gamma}$ is reduced by a factor of the order of 10, then the ω peak does not contribute appreciably and the ρ peak is too broad and flat to produce a large enough enhancement. This fact leads one to be pessimistic about observing the leptonic decays of the ρ and ω in this manner. Only if a 5% experiment with narrow resolution could be performed might one hope to see this effect.

ACKNOWLEDGMENT

The author wishes to thank Professors W.K.H. Panofsky and H. P. Noyes for their hospitality at SLAC, where most of this work was performed. Helpful discussions with Drs. Sidney Drell, Robert Mozley, and Darrell Drickey are also gratefully acknowledged.

NOTE ADDED IN PROOF

After this paper was finished the author was informed by Dr. S. Drell (Stanford Linear Accelerator Center) of some more recent data taken by the C.E.A. Group which indicates that the following modifications must be made in this argument:

1. The data for ρ-production seem to be less and less consistent with a peripheral model and show very significant diffraction contributions(F. Pipkin, private communication). This does not change the overall result of this paper, however, since this possibility is already dealt with in Sec. III.B.

2. The production cross section for ω-mesons now seems to be at least 25% of that for ρ-production. If we let χ equal the ratio $(g_{\omega\pi\gamma}/g_{\rho\pi\gamma})$, then we can account for whatever ω coupling is finally determined by multiplying our valve for R in Fig. 6 by $(1+\chi)^2$. [See also Eq. (7)]. Finally, we must qualify our statement at the end of Sec. IV to the effect that if the $\omega\pi\gamma$ coupling is indeed of the same order as the $\rho\pi\gamma$ coupling, the chances of seeing the ρ,ω bumps in the μ-pair spectrum are greatly enhanced.

FOOTNOTES AND REFERENCES

1. See for example S. D. Drell, Ann. Phys. 4, 75 (1958).
2. J. K. dePagter, et al., Phys. Rev. Letters, 12, 739 (1964).
3. R. F. Mozley (private communication).
4. For a more general treatment of the problem of lepton pair production on nuclear target, see S. D. Drell and J. D. Walecka, Ann. Phys. 28, 18 (1964).
5. J. D. Bjorken, S. D. Drell and S. C. Frautschi, Phys. Rev. 112, 1409 (1958).
6. L. N. Hand, D. G. Miller and R. Wilson, Rev. Mod. Phys. 35, 335 (1963).
7. Inelastic effects at the proton vertex have been neglected, but these can be included by modifying the form factors which appear in A and B.
8. cf., S. M. Berman and S. D. Drell, Phys. Rev. 133, B791, (1964). We have extended the Berman and Drell formula to allow for the virtual vector meson to be well off its mass shell.
9. H. R. Crouch, et al., Phys. Rev. Letters 13, 636 (1964).
10. C. C. Ting, L. W. Jones and M. L. Perl, Phys. Rev. Letters 9, 468 (1962).
11. See for example L. I. Schiff, Quantum Mechanics, (McGraw Hill, New York, 1955) p. 105.
12. This again is an overestimate based on a total cross section for photoproduction of ρ's of 30 μb. We do this because we want our estimates to still be large at photon energies of 10 BeV.
13. K. Gottfried and J. D. Jackson, Nuovo Cimento 34, 735 (1964).
14. M. Ross and G. L. Shaw, Phys. Rev. Letters 12, 627 (1964).

FIGURE CAPTIONS

1. "Bethe-Heitler" graphs for muon pair production.
2. General "Compton" graph.
3. Symmetric Bethe-Heitler cross section vs. lab angle of detected meson for various incident photon energies.
4. Breakdown of Fig. 2 into the S, t, u channels.
5. Peripheral production of mu-pairs.
6. Ratio of amplitude for peripheral production to amplitude for Bethe-Heitler production vs. invariant momentum transfer.
7. Approximation to form factor at $\rho\pi\gamma$ vertex.
8. Top rung of diffraction production graph.

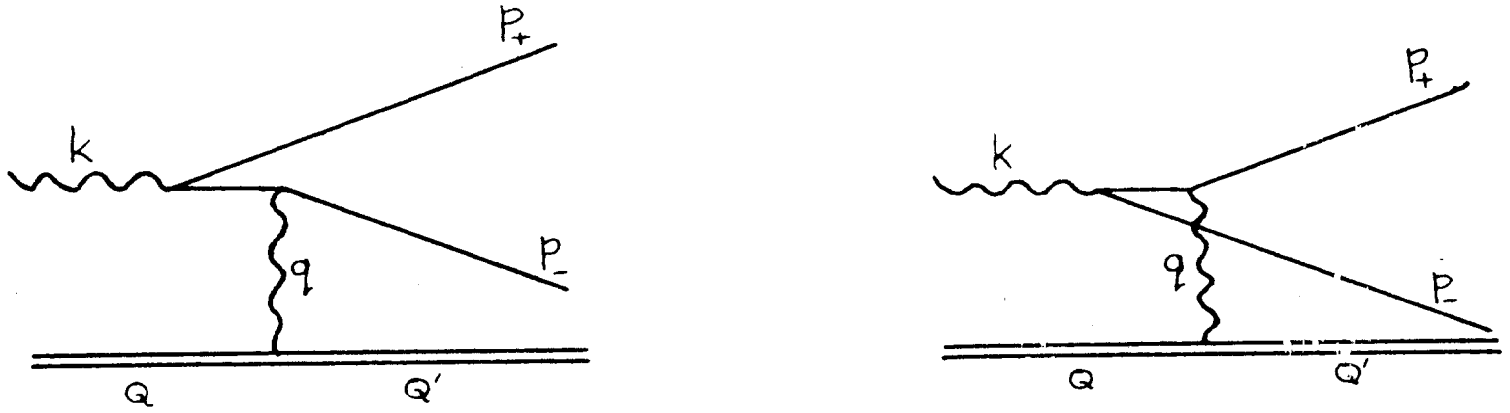

FIGURE 1

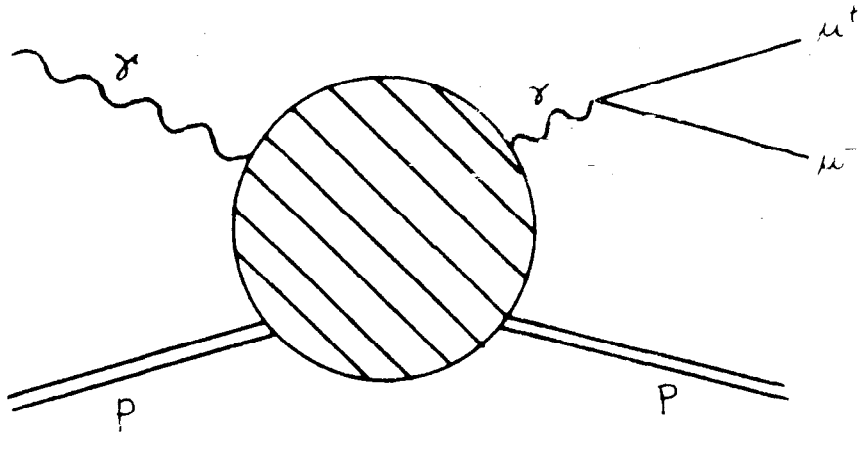

FIGURE 2

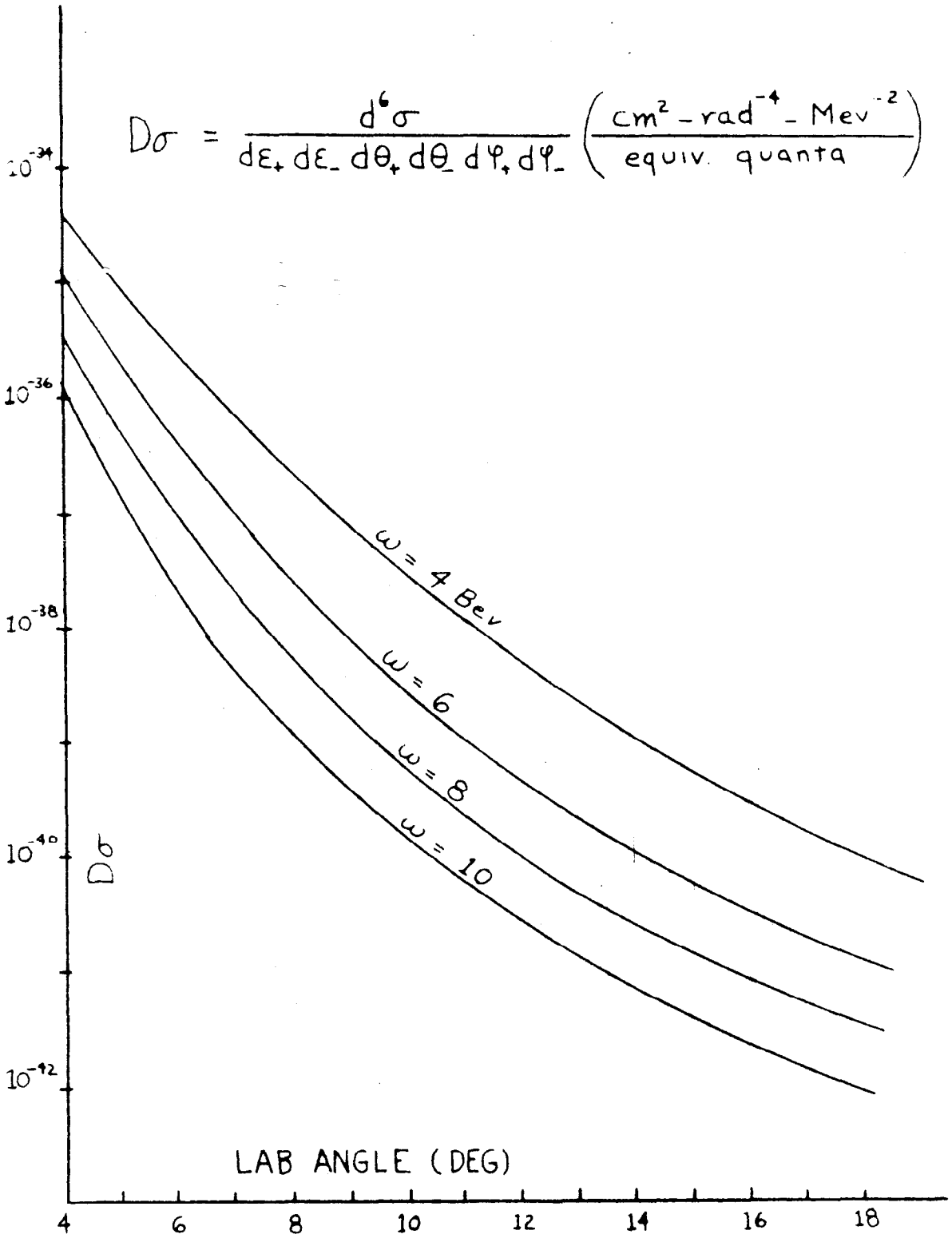
$D\sigma = \frac{d^6\sigma}{d\varepsilon_+ d\varepsilon_- d\theta_+ d\theta_- d\varphi_+ d\varphi_-} \left(\frac{cm^2 - rad^{-4} - Mev^{-2}}{equiv.\ quanta} \right)$
10^{-34}
10^{-36}
10^{-38}
10^{-40}
10^{-42}
$D\sigma$
$\omega = 4$ Bev
$\omega = 6$
$\omega = 8$
$\omega = 10$
LAB ANGLE (DEG)
4
6
8
10
12
14
16
18

FIGURE 3

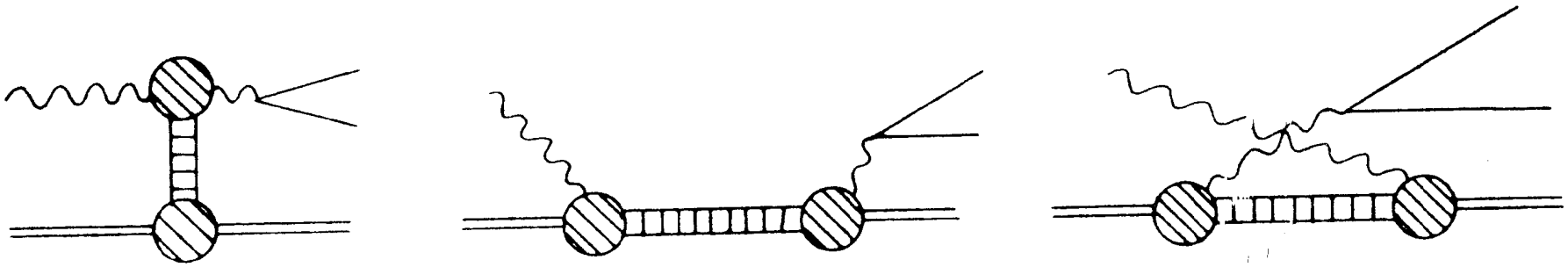

FIGURE 4

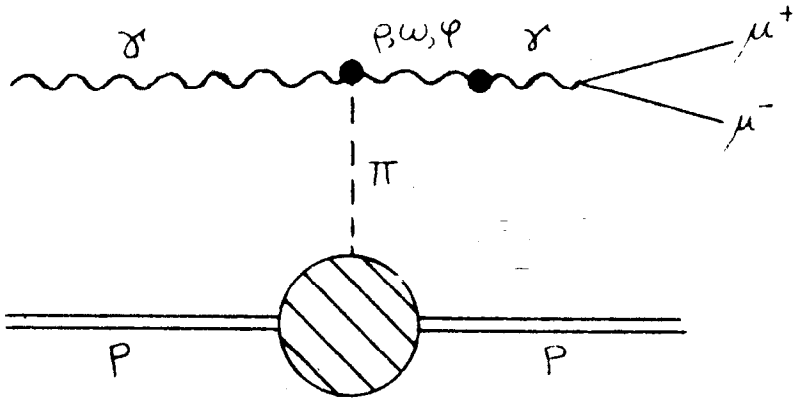

FIGURE 5

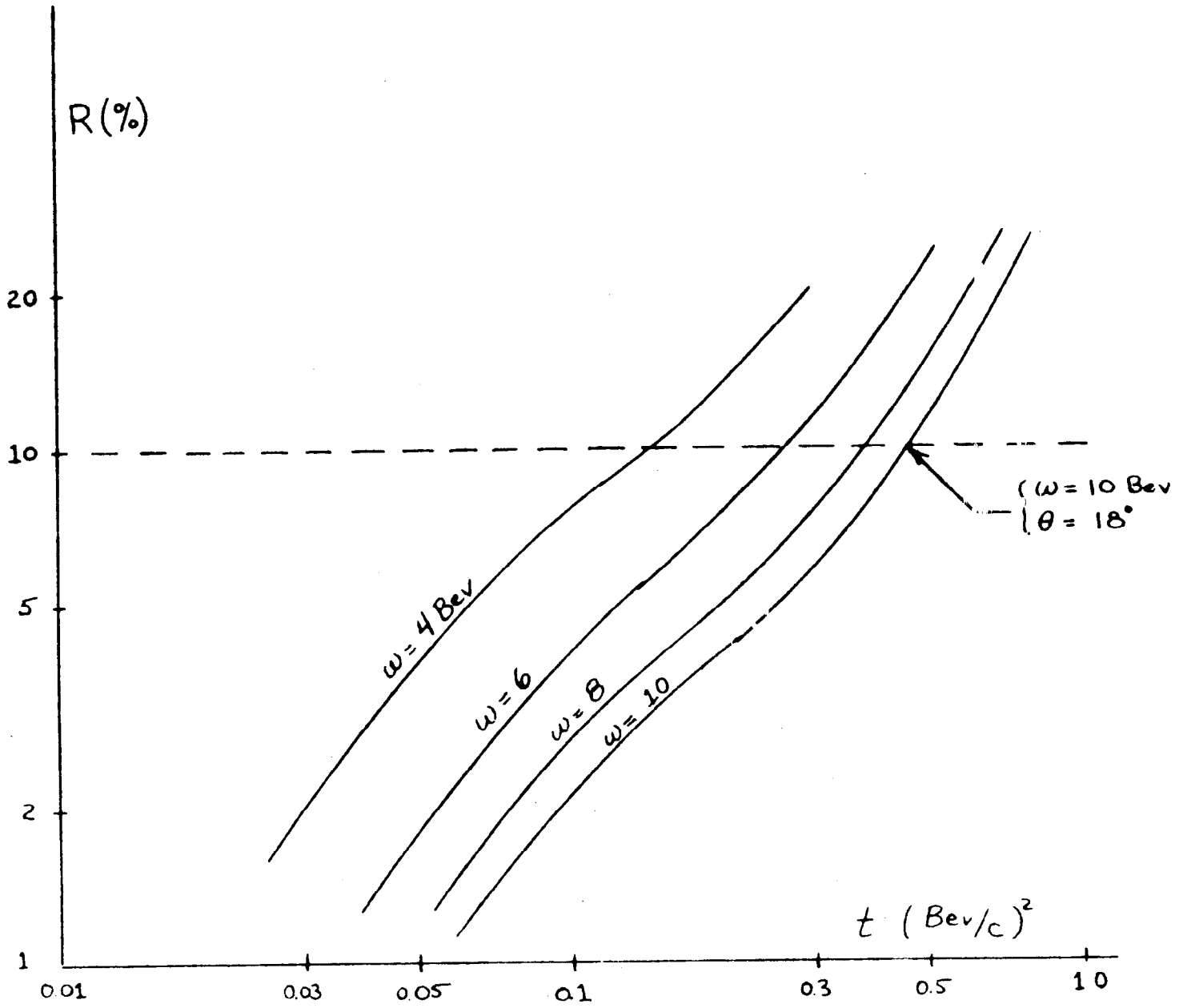
R(%)
20
10
5
2
1
0.01
0.03
0.05
0.1
0.3
0.5
1.0
t (Bev/c)²
ω = 4 Bev
ω = 6
ω = 8
ω = 10
ω = 10 Bev
θ = 18°

FIGURE 6

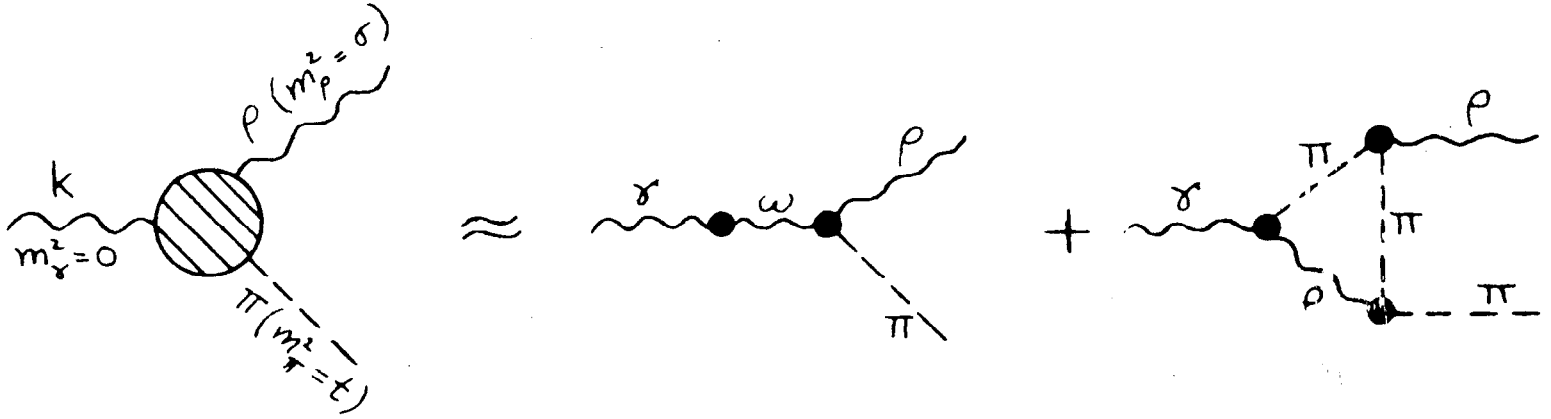
k
$m_\gamma^2 = 0$
$\rho\,(m_\rho^2 = \sigma)$
$\pi\,(m_\pi^2 = t)$
$\approx$
γ
ω
ρ
π
+
γ
π
ρ
π
ρ
π

FIGURE 7

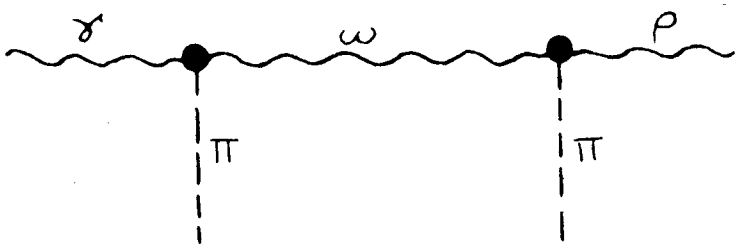

FIGURE 8